

# Laser cooling with adiabatic passage for diatomic molecules

Qian Liang,<sup>1</sup> Tao Chen,<sup>1,\*</sup> Wenhao Bu,<sup>1</sup> Yuhe Zhang,<sup>1</sup> and Bo Yan<sup>1,2,†</sup>

<sup>1</sup>*Department of Physics, State Key Laboratory of Modern Optical Instrumentation, Zhejiang University, Hangzhou, China, 300012*

<sup>2</sup>*Collaborative Innovation Centre of Advanced Microstructures, Nanjing University, Nanjing, China, 210093*

(Dated: May 29, 2022)

We demonstrate a magnetically enhanced laser cooling scheme applicable to multi-level type-II transitions and further diatomic molecules with adiabatic transfer. An angled magnetic field is introduced to not only remix the dark states, but also decompose the multi-level system into several two-level sub-systems in time-ordering, hence allowing multiple photon scattering as long as the Zeeman shift is sufficiently large. For complex 4+12 level diatomic molecules, we observe a  $\sim 4\times$  enhancement of the damping coefficient and a rather wide cooling velocity range compared to the conventional Doppler cooling. A reduced dependence on spontaneous emission of this scheme makes laser cooling systems with leakage channels become a feasibility.

## I. INTRODUCTION

First realized in atoms [1–3], laser cooling, as an excellent and powerful tool, has significantly revolutionized the development of the atomic, molecular, optical and quantum physics during last several decades [4–8]. Being simple and effective, conventional Doppler cooling only requires a light field with one single frequency. Some multi-frequency cooling schemes [9], such as adiabatic rapid passage [10–12] and bichromatic force [13–16], have been developed and predicted to show a better performance beyond the conventional case. However, since standard scheme is good enough for most atomic species, such techniques have not been widely used by increasing the complexity of the system. Nevertheless, these might be potentially applied into cooling molecules although some new features show up [17, 18]. First, the closed transition in molecules is not a trivial case. Molecules in excited states can decay to different vibrational states governed by the Franck-Condon factors [19, 20], which introduces leakage channels. Second, the energy levels for molecules are complex and type-II transitions dominate [21, 22], making the cooling process much more complicated and the achievable cooling force much weaker than atomic cases. To this end, it might worth to sacrifice the simplicity of the cooling scheme by introducing multiple frequencies [23] for a better cooling efficiency.

For conventional laser cooling, an atom-light interaction approach in either semi-classical or quantum picture can be directly applied to explain the momentum transfer [24–26]. The strength of the radiation force depends on how fast the momentum exchange is repeated, i.e., the decay rate from the excited state to the ground state. Once successive scattering in a closed cycling transition was achieved, the force would be eventually limited by the spontaneous emission rate  $\Gamma$ . For a two-level system, it is  $F_{\text{rad,max}} = \hbar k \Gamma / 2$  with  $\hbar k$  the photon momentum.

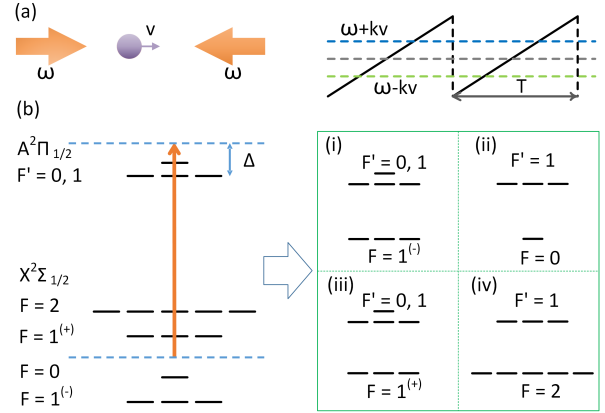


FIG. 1. (a) Laser cooling scheme with sawtooth wave adiabatic passage. The two counter-propagating laser beams with a frequency of  $\omega$  interact with a moving particle with a velocity of  $v$ . The laser frequency  $\omega$  ramps increasingly, and the sweeping period is  $T$ . Due to Doppler effect, the two beams get on-resonance with the moving particle at different time points. (b) Level structure for typical laser coolable diatomic molecules, only rotational, hyperfine and Zeeman branches are shown. The bottom dashed line indicates the center frequency position of the two chirped laser beams, and  $\Delta$  is the shift of the center frequency of the sweeping. Such a 4+12 system can be decomposed into four sub-systems as: (i)  $F = 1^{(-)} \rightarrow F' = 0, 1$ , (ii)  $F = 0 \rightarrow F' = 1$ , (iii)  $F = 1^{(+)} \rightarrow F' = 0, 1$  and (iv)  $F = 2 \rightarrow F' = 1$ . Only case (ii) is type-I transition while others are type-II transitions.

Alternatively, the temperature limit and cooling velocity range also depend on the decay rate [24].

In order to overcome the limit of spontaneous emission rates, stimulated emission can be used to perform laser cooling. Recently, an adiabatic-passage cooling scheme by rapidly sweeping the laser frequency in a sawtooth wave shape (SWAP) has been demonstrated in narrow-line transitions [27–29] and Raman transitions [30]. Since such a scheme uses a stimulated emission process to make the excited atoms back to the ground state, strong forces can be achieved with a high sweeping repetition rate

\* phytch@zju.edu.cn

† yanbohang@zju.edu.cn

even for narrow transitions. Let us consider a moving particle with a velocity of  $v$  in a light field from two counter-propagating laser beams with a frequency of  $\omega$ ; see Fig.1(a). Due to the Doppler effect, absorptions of the photons from the two beams are separated in time ordering. An increasing ramp in a sweeping period  $T$  introduces two photon momentum transfer to the atom in the opposite direction of  $v$ , resulting an average force of  $F_{\text{swap}} = 2\hbar k/T$ . To guarantee the adiabatic transfer, the Landau-Zener condition  $\Omega^2 \gg \alpha$  should be fulfilled [31], here  $\Omega$  is the on-resonance Rabi frequency for the two beams and  $\alpha$  is the ramp speed of the frequency sweeping.

Here, we extend the SWAP cooling scheme to type-II transitions and further molecules. Diatomic molecules which have been directly laser-cooled typically have a 4+12 level structure illustrated in Fig.1(b), and here the vibrational branches and other possible leakage channels have not been shown yet. Such a system can be simply decomposed into four sub-systems; and except type-I case (ii)  $F = 0 \rightarrow F' = 1$ , other three cases are all type-II transitions which usually show a much weaker cooling force [32, 33] due to the remixing process of the Zeeman dark states by either rapidly switching the polarization of the laser beams [18, 34] or introducing an angled magnetic field to redefine the quantum axis [17, 35]. In the following, we consider the latter case and show that a large magnetic field can also enhance the momentum transfer in the scattering event.

## II. COOLING EFFECT ON MULTI-LEVEL TYPE-II TRANSITIONS.

We employ a time dependent master equation approach to investigate the interaction between a multi-level system with a frequency chirped laser field; see Appendix A. Let us first consider the simplest type-II  $F = 1 \rightarrow F' = 0$  transition under a magnetic field with an angle  $\theta = \pi/2$  to the laboratory  $z$ -axis (see the definitions in Appendix B). The counter-propagating laser beams are in  $\sigma^+ - \sigma^-$  configuration, which covers all possible transitions after a transformation according to local quantum axis determined by the angle  $\theta$ . With different magnetic field strength, the cooling force shows rather different behaviours, as shown in Fig.2(a). Compared to the conventional Doppler cooling where the maximum achievable cooling force approximates  $\sim 0.06\hbar k\Gamma$ , the SWAP cooling scheme, even under a weak magnetic field strength of  $B = 10$  G, shows a stronger cooling ability and a wider cooling range to tens of  $\Gamma/k$  [ $k$  is the wavevector of the cooling laser]. Increasing the magnetic field strength results in that the velocity range with a force larger than  $0.1\hbar k\Gamma$  becomes extended, although the maximum cooling force dose not change a lot,  $\sim 0.6\hbar k\Gamma$ , ten times larger than that in the conventional case. One reason for such a stronger cooling effect in small velocity region should be resorted to the non-trivial Bragg oscilla-

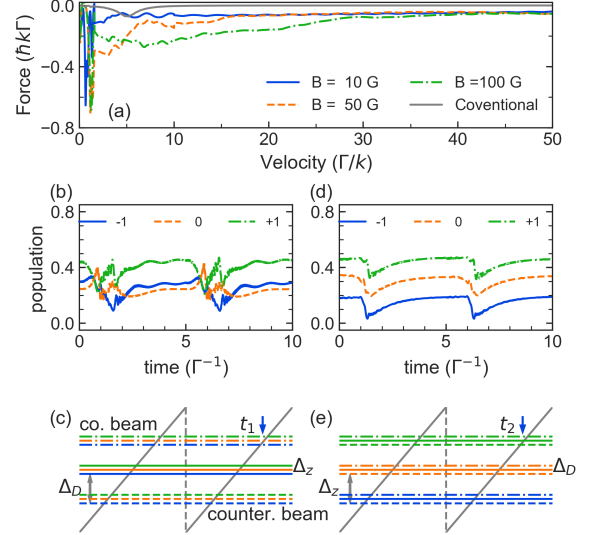


FIG. 2. (color online) Effect of the SWAP cooling on the type-II  $F = 1 \rightarrow F' = 0$  transition. The on-resonance Rabi frequency  $\Omega = 50\Gamma$ , the frequency ramp speed  $\alpha = 100\Gamma^2$  and sweeping period  $T = 5\Gamma^{-1}$ . The Landé  $g$ -factor of the ground state is  $g_F = -0.5$ . (a) Comparison of the SWAP cooling forces under various magnetic field strengths. The conventional case (gray solid line) is calculated with the Rabi frequency  $\Omega = 2\Gamma$ , detuning  $\Delta = -5\Gamma$ , angled magnetic field  $B = 5$  G ( $\theta = \pi/2$ ). (b) Time evolution of the populations in the three Zeeman sublevels of the ground  $F = 1$  state after the system reaches the quasi-steady state. The moving velocity  $v = 80\Gamma/k$  and the magnetic field strength  $B = 10$  G, that is, the Doppler detuning  $\Delta_D$  is much larger than the Zeeman detuning  $\Delta_z$ . (c) The frequency sweeping scheme for the case in (b) (not to scale). The solid horizontal lines indicate the resonant point of the three sublevels with the frequency-chirped laser beams, and the vertical separation is the Zeeman detuning  $\Delta_z$ . Due to the Doppler effect (detuning of  $\Delta_D$ ), the counter-propagating beam first gets on-resonance and then the co-propagating beam around time point  $t_1$ . The resonant frequencies are illustrated with dashed lines and dotted dashed lines for the two beams respectively. The orange, green and blue colors correspond to the three sublevels in (b) respectively. (d) Time evolution of the ground populations under the condition with  $v = 2\Gamma/k$  and  $B = 100$  G such that  $\Delta_z \gg \Delta_D$ . The evolutions for each sublevels are nearly independent from each other. (e) The resonant position of each polarization component in the two beams. The colors and line styles have the same identifications with those in (c).  $t_2$  is the time point where the  $\sigma^-$  components of the both beams are near resonant with the moving particle.

tions that induce more than  $2\hbar k$  of momentum transfer in one sweeping period even for a two-level system, as discussed in Ref.[31].

Besides the Bragg oscillation effect, a new mechanism induces rather different cooling behaviors for large and small velocities in a multi-level system. The force strength depends on a competition between the stimulated emission (excitation) process and the  $\Lambda$ -type tran-

sitions. For a large moving velocity, for example,  $v = 80\Gamma/k$ , the Doppler detuning  $\Delta_D = kv$  is much larger than the Zeeman splitting  $\Delta_z = \mu g_F B/\hbar$ , let us consider a time point  $t_1$  [in Fig.2(c)] where the frequency of the co-propagating beam which contains three polarization components becomes near resonant with the moving particle. At  $t_1$ , the particles in the excited state begin to be transferred back to the  $m_F = -1$  sublevel via stimulated emission, inducing a population imbalance between the three Zeeman sublevels. However, since the Zeeman splitting is small while the on-resonance Rabi frequency  $\Omega \gg \Delta_z$ , the other  $\pi$  and  $\sigma^-$  components play a significant role and population transfer from  $m_F = -1$  to other two sublevels happens, as we can clearly see the oscillation of the populations in the three Zeeman sublevels in the  $F = 1$  ground state in Fig.2(b). The photon scattering in the two processes gets canceled with each other. Such  $\Lambda$ -type transitions break up the stimulated emission, similar to the  $V$ -type transitions in type-I  $F = 0 \rightarrow F' = 1$  system as discussed in Appendix C, and consequently the cooling force is weak, even smaller than the conventional maximum achievable cooling force,  $0.25\hbar k\Gamma$ , predicted by the analytical result of the scattering rate from the rate equations [36].

However, in the small velocity region where  $\Delta_D \ll \Delta_z$ , the stimulated excitation and emission processes dominate, leading to a larger cooling force. Figure 2(d) gives the time evolutions of the populations in the ground three Zeeman sublevels when the system reaches the quasi-steady state. It is clear that the three sublevels evolve almost independently and only a small delay in time occurs as both  $\Omega$  and  $\alpha$  are large enough. The physical picture can be easily understood from Fig.2(e). The large magnetic field strength results in that the three sublevels become resonant with the corresponding polarization components in the two laser beams at different time during one sweeping period. Then, such a 1+3 system can be treated as three two-level sub-systems. For example, at time  $t_2$  [in Fig.2(e)], the  $\sigma^-$  components in the counter-propagating beam and co-propagating beam drive the stimulated excitation and emission processes respectively, and two-photon momenta are transferred. So as long as the magnetic field is strong enough, such three two-level sub-systems allow transferring a momentum of  $3 \times 2\hbar k$ , leading to a maximum achievable cooling force of  $\sim 6\hbar kT^{-1}$ . However, in practice, due to the large value of  $\Omega$ , the  $\Lambda$ -type transitions can not be perfectly weakened even with  $B = 100$  G [ $\Delta_z \sim 25\Gamma$ ], and thus the force can not reach  $1.2\hbar k\Gamma$  with  $T = 5\Gamma^{-1}$ . On the other hand, although stronger magnetic field strength is better to make the three two-level sub-systems separated far from each other, the upper limit of the strength is constrained by the frequency sweeping range  $\Delta_T$ , i.e.,  $2\Delta_z < \Delta_T (= \alpha T)$ . Here we conclude that, for a finite sweeping period, larger  $B$  requires rapider ramp speed  $\alpha$  which should fulfill the adiabatic condition  $\alpha \ll \Omega^2$ .

This enhanced cooling mechanism is universal and of course validates for other type-II transitions in Fig.1(b).

The maximum achievable cooling force is about 5 times larger than that in conventional Doppler cooling; see Appendix D. Besides, the robustness of the SWAP cooling scheme for type-I  $F = 0 \rightarrow F' = 1$  under a static magnetic field in Appendix C indicates the feasibility of enhanced laser cooling effect for molecules, and here we take the BaF molecule as an example.

### III. SWAP COOLING ON DIATOMIC MOLECULES.

Figure 3(a) gives a comparison between the cooling force in the SWAP scheme and that from the conventional Doppler cooling for diatomic molecules, and an enhancement is clearly illustrated. In the small velocity region,  $v < 5\Gamma/k$ , i.e., less than  $\sim 15$  m/s for the BaF molecule, the cooling force does not behave like those for the four sub-systems discussed above and the enhancement is not as significant as those as well. The reason lies in that the energy gaps of the four hyperfine states typically are tens of  $\Gamma$  and some  $\Lambda$ -type transitions due to the Zeeman splitting still limit the photon scattering (see Appendix E). For example, under a magnetic field of 100 G, the sublevels  $|F = 1^{(+)}, m_F = -1\rangle$  and  $|F = 1^{(-)}, m_F = 0\rangle$  are near degenerate, resulting in that the stimulated excitation and emission processes are depressed by the population transfer between such paired states even for a rather small velocity. A linear fit of the cooling force  $F$  versus the velocity  $v$  with  $F = -\beta mv$  [ $m$  is the mass of the molecule] tells us the damping coefficient  $\beta$  for the SWAP cooling; see Fig.3(a). According to the Fokker-Planck kinetic theory [24], the cooling temperature limit  $T_{\text{lim}} \propto \beta^{-1}$ . For conventional Doppler cooling of the BaF molecule with typical parameters and a 38 MHz sideband modulation,  $\beta \sim 1000 \text{ s}^{-1}$ ; while a three times larger  $\beta \sim 3500 \text{ s}^{-1}$  can be yielded with the SWAP scheme. This indicates that a lower temperature might be obtained, although the momentum diffusion coefficients due to the fluctuations of the cooling force for the two schemes are different.

The dependence of the damping coefficient  $\beta$  on the parameters of the frequency chirped cooling laser is shown in Figs.3(b)-(d). For a fixed frequency ramp speed  $\alpha$ , the damping coefficient  $\beta$  rises proportionally with the on-resonance Rabi frequency  $\Omega$  within the adiabatic condition  $\Omega^2 \gg \alpha$ ; see Fig.3(b). It is clear that value of  $\beta$  in the SWAP cooling becomes larger than that of the conventional Doppler cooling with typical parameters when  $\Omega^2 > 25\alpha$ . This critical condition also validates on the SWAP cooling force for large velocities, for example,  $v = 50\Gamma/k$ , as shown in Fig.3(e). When  $\Omega^2 > 50\alpha$ , the enhancement of the SWAP cooling force by increasing  $\Omega$  is not significant yet for both medium velocity  $v = 10\Gamma/k$  and large velocity  $v = 50\Gamma/k$ . Apparently, an enhanced cooling effect for larger velocity requires a stronger laser intensity, which is an important issue to be considered if one expects using the SWAP scheme to achieve laser

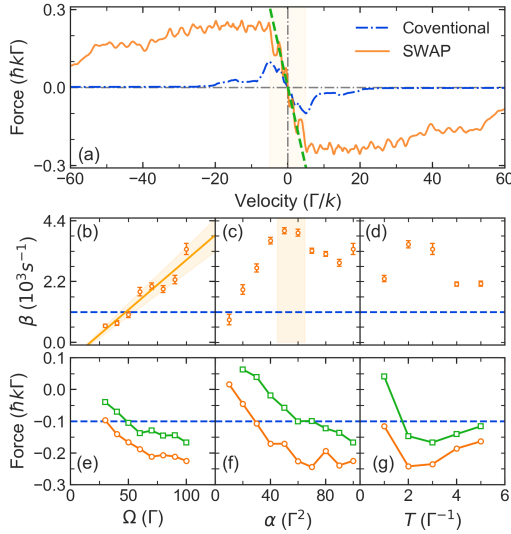


FIG. 3. (color online) The SWAP cooling on the 4+12 level diatomic molecule. Here we use the parameters of the BaF molecule. (a) Comparison between the SWAP cooling (orange solid line) and the conventional Doppler cooling (blue dotted dashed line). For the SWAP cooling,  $\Omega = 100\Gamma$ ,  $\alpha = 100\Gamma^2$ ,  $B = 100$  G,  $T = 3\Gamma^{-1}$ . The parameters used in the conventional cooling are  $\Omega = 5\Gamma$ ,  $\Delta = -5\Gamma$ ,  $B = 5$  G and a 38 MHz sideband modulation to the cooling laser also applied to cover all hyperfine levels [22]. A linear fit (green dashed line) to the shaded small velocity region gives the damping coefficient  $\beta$ . (b)-(d) Dependence of  $\beta$  on the on-resonance Rabi frequency  $\Omega$ , ramp speed  $\alpha$  and sweeping period  $T$  respectively in SWAP cooling. The blue dashed lines indicate the  $\beta$  value from the conventional Doppler cooling in (a). In (b), the solid line is a linear fit to the data points and the shadow indicates the fitting standard error. (e)-(g) Dependence of the cooling forces for specific velocities,  $v = 10\Gamma/k$  (orange circle) and  $v = 50\Gamma/k$  (green square), on the on-resonance Rabi frequency  $\Omega$ , ramp speed  $\alpha$  and sweeping period  $T$  respectively. The blue dashed line indicate the maximum force value achieved from Doppler cooling scheme.

slowing of a molecular beam.

Figure 3(c) shows the dependence of  $\beta$  on the frequency ramp speed  $\alpha$  for a fixed on-resonance Rabi frequency  $\Omega = 100\Gamma$  and sweeping period  $T = 3\Gamma^{-1}$ . A value of  $\alpha$  around  $\sim 50\Gamma^2$  results in a maximum value of  $\beta \sim 4000 s^{-1}$ , about  $\sim 4\times$  larger than that for the conventional Doppler cooling. Although decreasing  $\alpha$  makes the adiabatic condition better fulfilled, the SWAP cooling force for large velocities gets weakened and even heating occurs; see Fig.3(f). However, for a medium velocity, for example,  $v = 10\Gamma/k$ , the force increases to a saturated value of  $\sim 0.25\hbar k\Gamma$  by increasing  $\alpha$ , and consequently, a larger  $\alpha$  might not be necessary yet if we only pay attention to the velocity region with a medium upper limit in laser cooling experiments.

Figure 3(d) illustrates how  $\beta$  varies with different sweeping period  $T$  for fixed  $\Omega = 100\Gamma$  and  $\alpha = 100\Gamma^2$ . It is clear that the sweeping period  $T$  had better not

be too large or too small with an optimal value around  $2 \sim 3\Gamma^{-1}$ . The cooling forces for large velocities exhibit a similar behavior, as shown in Fig.3(g). The reason why smaller cooling forces are obtained with smaller  $\alpha$  and  $T$  is that blue detuning always maintains in the  $F = 2 \rightarrow F' = 1$  sub-system for any frequency within the sweeping range; see Appendix E. If we temporarily neglect the Zeeman splitting, with a rather small  $\alpha = 10\Gamma^2$  while keeping  $T = 3\Gamma^{-1}$ , the sub-system  $F = 1^{(+)} \rightarrow F' = 1, 0$  is always blue detuning as well, and heating phenomenon appears although other two sub-systems keep red detuned. So the sweeping effect is masked and meaningless for a small sweeping range. Larger  $T$  induced weak cooling force can be understood from the definition of the force by scattering  $N_{ph}$  photons per period, i.e.,  $F = N_{ph}\hbar k/T$ . For a sufficient large  $T$ ,  $N_{ph}$  does not change significantly and smaller repetition rates apparently lead to weaker forces.

On the other hand, the SWAP cooling force has a weak velocity selective character, as shown in Fig.3(a), and the cooling velocity region below a critical value  $v_c$  is determined by the frequency sweeping range  $\Delta_T$  and the magnetic field strength  $B$ . The enhancement of the cooling force does not happen otherwise the frequency sweeping range cover all possible sublevels in the 4+12 system. Considering both the Doppler shift and Zeeman shift, we have

$$2kv + 2|\Delta_z^{(F=2)}| + |\Delta_z^{(F=1^{(-)})}| + \Delta_{hf} < \Delta_T, \quad (1)$$

which can only give an empirical value of the critical velocity,  $v_c$ , with specific parameters of the chirped lasers. Here  $\Delta_{hf} \approx 56\Gamma$  is the energy gap between the two hyperfine states  $F = 2$  and  $F = 1^{(-)}$  for the BaF molecule [20].

Similar to the discussions on the magnetic field in  $F = 1 \rightarrow F' = 0$  transition, Eq.(1) tells us that the upper limit of the field strength  $B_u$  depends on the frequency sweeping range  $\Delta_T = \alpha T$ . Let us consider the cooling

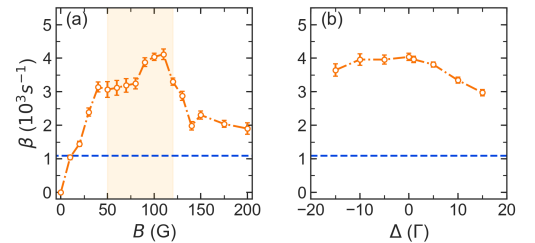


FIG. 4. The damping coefficient  $\beta$  of the SWAP cooling force on the 4+12 level diatomic molecule as functions of: (a) angled magnetic field strength  $B$  ( $\theta = \pi/2$ ) and (b) shift  $\Delta$  of the center frequency in a sweeping period. Here we use the parameters of the BaF molecule and the on-resonance Rabi frequency  $\Omega = 100\Gamma$ , the frequency ramp speed  $\alpha = 50\Gamma^2$ , the sweeping period  $T = 3\Gamma^{-1}$ . In (a),  $\Delta = 0$ , while in (b),  $B = 100$  G. The blue dashed lines indicate the  $\beta$  value from the conventional Doppler cooling scheme used in Fig.3(a).



effect in small velocity region, i.e., how the damping coefficient  $\beta$  varies with different values of  $B$ ; see Fig.4(a). With the sweeping parameters used there and neglecting the Doppler shift as  $v$  is small, we have  $B_u \sim 120$  G from Eq.(1). Our calculation results demonstrate this by witnessing a rapid decrease of  $\beta$  value with an increasing of magnetic field strength larger than  $B_u$  in Fig.4(a). The lower limit of the magnetic field,  $B_l$ , is determined empirically as well. Whether the SWAP cooling force in small velocity region ( $v < v_0 = 5\Gamma/k$ ) gets enhanced or not depends on the competition between the stimulated excitation (emission) process and the  $\Lambda(V)$ -type transitions. To make the stimulated processes dominate, the magnetic field strength  $B$  should be larger enough, and here we empirically choose  $\mu B/\hbar > 10kv_0$ , leading to  $B_l \sim 50$  G. From Fig.4(a), the enhancement of  $\beta$  value with a magnetic field strength beyond the interval  $[B_l, B_u]$  is less significant than those within.

We have also checked the robustness of the SWAP cooling force on the shift of the center frequency in a sweeping period, as shown in Fig.4(b). Even with a rather large shift,  $|\Delta| = 15\Gamma$ , about  $\sim 40$  MHz for the BaF molecule, the damping coefficient  $\beta$  slightly changes and is still larger than  $3000 \text{ s}^{-1}$ . This indicates that the long-term stabilization of the cooling laser might not be strictly fulfilled, contrasting to the conventional Doppler cooling where the detuning should be precisely controlled at a magnitude of  $\sim \text{MHz}$  [37]. Furthermore, we should take into account the experimental realization of the large on-resonance Rabi frequency  $\Omega = 100\Gamma$  and rapid sweeping with a ramp speed of  $\alpha = 50\Gamma^2$ . For narrow linewidth transitions, i.e.,  $\Gamma \sim \text{kHz}$ , the frequency sweeping can be easily achieved with an acousto-optic modulator [28, 29] and the laser intensity required is not too extreme. However, once extending to transitions with  $\Gamma \sim \text{MHz}$ , for example, the BaF molecule being investigated, the saturated intensity  $I_s \sim 0.58 \text{ mW/cm}^2$  and an  $\Omega = 100\Gamma$  indicates a rather high laser intensity of  $\sim 10 \text{ W/cm}^2$ . On the other hand, the frequency ramp speed  $\alpha = 50\Gamma^2$  corresponds to  $\sim 2.5 \text{ MHz/ns}$ , which can be realized with an electro-optical modulator and the injection locking technique in Refs.[38, 39] where a ramp speed of  $\sim 100 \text{ MHz/ns}$  was yielded.

#### IV. RESISTANCE TO LEAKAGE CHANNELS

For molecules, the closed cycling transitions, i.e., the 4+12 levels in Fig.1(b), usually can not be perfectly realized due to the leakage channels, such as the higher vibrational states and the intermediate  $\Delta$  state [20, 40]. Since the SWAP cooling scheme employs the stimulated emission to transfer the excited particles back to the ground state, the fraction of spontaneous decay gets partly suppressed. Hence, compared to the conventional Doppler cooling, a smaller loss to the possible leakage channels might be expected. In order to get some idea of such effect, we consider a simple three-level system, i.e., a two-

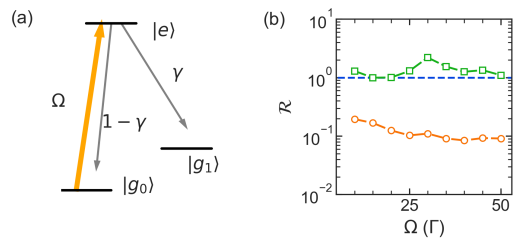


FIG. 5. The SWAP cooling effect on the leakage channels. (a) A schematic plot of a two-level system  $|g_0\rangle \rightarrow |e\rangle$  driven by a pair of cooling laser beams (on-resonance Rabi frequency  $\Omega$ ) with an additional leakage channel  $|g_1\rangle$ . The leakage rate is  $\gamma$ . (b) The dependence of the loss ratio  $\mathcal{R}$  of the SWAP cooling on the on-resonance Rabi frequency  $\Omega$  for the small ( $v = 2\Gamma/k$ , orange circles) and large ( $v = 20\Gamma/k$ , green squares) velocities. Here,  $\alpha = 20\Gamma^2$ ,  $T = 10\Gamma^{-1}$ .

level transition driven by the frequency-chirped cooling lasers with an additional loss channel; see Fig.5(a). In the conventional Doppler cooling, a loss rate  $\gamma = 0.05$  allows a maximum scattering photon number of  $\gamma^{-1} \sim 20$  before the particle totally populates the leakage channel. In the SWAP cooling, with an evolution time of five sweeping periods, the population loss  $\ell_{\text{swap}}$  is several times lower than that in Doppler cooling, and the loss fraction is nearly linear to the number of the sweeping period before the cooling dies; see Appendix F for details.

To evaluate the resistance of the SWAP cooling to the loss, we introduce a loss ratio defined by  $\mathcal{R} = r_{\text{swap}}/r_{\text{conv}}$ . Here  $r_{\text{swap}}$  indicates the population loss in the SWAP cooling once the moving particle changing its momentum by  $-\hbar k$ , resulting a definition as  $r_{\text{swap}} = \ell_{\text{swap}}\hbar k/\delta p_{\text{swap}}$  with  $\delta p_{\text{swap}}(\tau) = |\int_0^\tau \langle F(t) \rangle dt|$  for an evolution time of  $\tau$ . In the conventional Doppler cooling,  $r_{\text{conv}} \sim \gamma$ . Figure 5(b) shows the loss ratios  $\mathcal{R}$  for two different velocities with various on-resonance Rabi frequency  $\Omega$ . For a large velocity, for example,  $v = 20\Gamma/k$ , the ratio always larger than one, which means that the cooling effect of the SWAP cooling is less significant than the conventional Doppler case as less momenta ( $\sim 10$  photons for five periods) are transferred but the loss lies in a similar or larger level. However, for a small velocity,  $v = 2\Gamma/k$ , the ratio is typically around  $\sim 0.1$ . The SWAP cooling introduces more than  $2\hbar k$  momentum transfer during one sweeping period due to the nontrivial Bragg oscillations. This is consistent with the effective condition  $|kv| \ll \Omega$  where the Bragg oscillations work [31]. Meanwhile, with a better fulfillment of the adiabatic condition  $\Omega^2 \gg \alpha$  by increasing  $\Omega$ , the ratio  $\mathcal{R}$  decreases, as shown Fig.5(b). As a result, we claim here that, compared to the conventional Doppler cooling, a better resistance to the leakage channels in the SWAP cooling only occurs in the small velocity region, i.e.,  $|v| < \Omega/k$ . To slow a molecular beam with a large velocity, a sufficient large laser intensity might be required to enhance the stimulated emission processes.

## V. CONCLUSION

In summary, we demonstrate the applicability of the SWAP cooling scheme for multi-level type-II transitions and further much more complex diatomic molecules. The angled magnetic field can not only remix the Zeeman dark states in the type-II transitions, but also introduce a new mechanism to enhance the SWAP cooling effect which depends on the competition between the stimulated processes and the  $\Lambda$ -type transitions. When the magnetic field is sufficient large, the Zeeman splitting is larger than the Doppler shift, the multi-level system can be decomposed into several two-level sub-systems as the resonant points for the Zeeman sublevels are separated in time ordering during one sweeping period, inducing multiple photons scattered and naturally an enhanced cooling force. Although the effect from the  $\Lambda$ -type transitions can not be totally suppressed in the diatomic molecules due to the energy gaps among the four

hyperfine states, we still observe a  $\sim 4\times$  enhancement of the damping coefficient in the small velocity region for the SWAP cooling and the cooling force can be rather strong even for a velocity upper to  $\sim 100$  m/s. Compared with the conventional Doppler cooling, such properties indicate a lower achievable cooling temperature and applications in laser slowing of a molecular beam. Finally, we have checked the resistance of the SWAP cooling to the leakage channels, opening the door of laser cooling an ordinary molecule that lacks a closed-cycling transition.

## ACKNOWLEDGMENTS

We acknowledge the support from the National Key Research and Development Program of China under Grant No.2018YFA0307200, National Natural Science Foundation of China under Grant No. 91636104, Natural Science Foundation of Zhejiang province under Grant No. LZ18A040001, and the Fundamental Research Funds for the Central Universities.

## Appendix A: Time dependent density matrix approach

Let us consider a one-dimension cooling of a multi-level particle in a multi-frequency laser field. An arbitrary multi-frequency light field can be decomposed as

$$\vec{E} = \sum_{p,q} \frac{1}{2} E_p \mathcal{E}_{pq} \hat{\epsilon}_q e^{i\vec{k}_p \cdot \vec{r}} e^{i\omega_p t} + h.c., \quad (\text{A1})$$

where  $p$  is the laser beam index for every frequency  $\omega_p$  and every wave vector (propagating direction)  $\vec{k}_p$  and the amplitude of the  $p$ -th beam is  $E_p$ ,  $q$  labels different laser polarizations and  $q = 0, \pm 1$  corresponds to  $\pi, \sigma^\pm$  components respectively, and the polarization vectors  $\hat{\epsilon}_0 = \hat{e}_z$ ,  $\hat{\epsilon}_\pm = \mp(\hat{e}_x \pm i\hat{e}_y)/\sqrt{2}$  in coordinate axis.  $\mathcal{E}_{pq}$  is the fractions for each polarization in the  $p$ -th beam.

Using Eq.(A1), the Hamiltonian under interaction picture reads as

$$H = \frac{\hbar}{2} \sum_{i,j} \sum_q \Omega_{ij}^{(q)} |j\rangle \langle i| + h.c. \quad (\text{A2})$$

with  $|i\rangle$  and  $|j\rangle$  indicate Zeeman sublevels  $|F, m_F\rangle$  and  $|F', m'_F\rangle$  in ground and excited states respectively, and

$$\Omega_{ij}^{(q)} = \sum_p e^{i\vec{k}_p \cdot \vec{r}} e^{-i\Delta_{pq}^{ij}(t)t} \mathcal{E}_{pq} \mathcal{A}_{ij}^{(q)} \Omega_p. \quad (\text{A3})$$

Here the detuning  $\Delta_{pq}^{ij}(t) = \omega_p(t) - \omega_{ij} + \delta_{ij}^{(B)}$  with  $\omega_p(t)$  in a sawtooth shape shown in Fig.1(a),  $\omega_{ij}$  the resonant frequency for  $|i\rangle \rightarrow |j\rangle$  transition, and the Zeeman detuning  $\delta_{ij}^{(B)} = \mu_B B (g_F m_F - g_{F'} m'_F)$  with  $\mu_B$  the Bohr magneton,  $B$  the external magnetic field,  $g_{F(F')}$  the Landé  $g$ -factor for the ground (excited) state. For atoms, the parameter  $\mathcal{A}_{ij}^{(q)}$  is the CG coefficients, i.e.,  $\langle F, m_F; 1, q | F', m'_F \rangle$ . For molecules, due to the state mixing, the  $\mathcal{A}_{ij}^{(q)}$  can be resolved from calculating the matrix elements for the electric dipole transition; for details, see the derivations in Ref.[20]. The total on-resonance Rabi frequency for the  $p$ -th beam is  $\Omega_p = E_p \langle F || \hat{d} || F' \rangle = \sqrt{s_p}/2\Gamma$  where  $\hat{d}$  is the electrical dipole moment,  $s_p$  is the saturated factor and  $\Gamma$  is the linewidth of the excited state.

The force from the interactions with the light field can be expressed as a gradient of the total energy of the system, that is,

$$\hat{F} = -\nabla H = -\hbar \sum_{i,j} \sum_q (\nabla \Omega_{ij}^{(q)}) |j\rangle \langle i| + h.c., \quad (\text{A4})$$

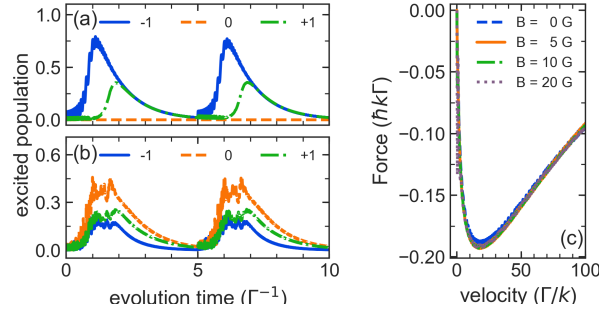


FIG. 6. Robustness of the SWAP cooling scheme to the magnetic field for the type-I  $F = 0 \rightarrow F' = 1$  transition. The on-resonance Rabi frequency  $\Omega = 50\Gamma$ , the frequency ramp speed  $\alpha = 100\Gamma^2$  and sweeping period  $T = 5\Gamma^{-1}$ . Time evolutions of the populations in each magnetic sublevel of the  $F' = 1$  excited state are shown in (a) without an angled magnetic field, while in (b) with an angled magnetic field of  $B = 5$  G and  $\theta = \pi/2$ . The moving velocity is  $v = 40\Gamma/k$ . (c) The dependence of the average cooling force during one sweeping period on the moving velocity under different magnetic field strength. The trajectory of the force slightly changes even under a strong magnetic field.

then the expectation value of the force for a system represented by a density matrix  $\rho$  can be yielded as  $\langle F \rangle = \text{Tr}(\rho \hat{F})$ . The time evolution of the density matrix  $\rho$  relying on the time dependent Hamiltonian is determined by the master equation

$$\frac{\partial \rho}{\partial t} = \frac{1}{i\hbar} [H(t), \rho] + \frac{1}{2} \sum_{ij} (2C_{ij}\rho C_{ij}^\dagger - C_{ij}^\dagger C_{ij}\rho - \rho C_{ij}^\dagger C_{ij}), \quad (\text{A5})$$

with the collapse operator  $C_{ij} = \sum_q \mathcal{A}_{ij}^q \sqrt{\Gamma} |i\rangle \langle j|$ .

## Appendix B: Transformation of the polarization fraction vector under an angled magnetic field

For type-II transitions and molecules, an external angled magnetic field  $B$  should be introduced to remixing the Zeeman sublevels. The direction of the magnetic field redefines the local quantum axis, and we assume the field on the coordinate  $yz$  plane with an angle of  $\theta$  to the  $z$  axis. The new fraction vector for the three polarizations in each laser beam can be transformed from the old one, i.e.,

$$\begin{pmatrix} \mathcal{E}'_{+1} \\ \mathcal{E}'_0 \\ \mathcal{E}'_{-1} \end{pmatrix} = \frac{1}{2} \begin{pmatrix} 1 + \cos \theta & \sqrt{2} \sin \theta & 1 - \cos \theta \\ -\sqrt{2} \sin \theta & 2 \cos \theta & \sqrt{2} \sin \theta \\ 1 - \cos \theta & -\sqrt{2} \sin \theta & 1 + \cos \theta \end{pmatrix} \begin{pmatrix} \mathcal{E}_{+1} \\ \mathcal{E}_0 \\ \mathcal{E}_{-1} \end{pmatrix}. \quad (\text{B1})$$

## Appendix C: Robustness of the SWAP cooling under static magnetic field for type-I transitions

The type-I  $F = 0 \rightarrow F' = 1$  magnetic optical trap under SWAP scheme has been demonstrated in the  $^1S_0 \rightarrow ^3P_1$  transition of Sr atom [28], where a magnetic field gradient was applied to generate the restoring force. Here we consider the cooling effect under an angled static magnetic field, since the four sub-systems in molecules can not be treated independently and other type-II transitions require the magnetic field to remix the Zeeman dark states. Figure 6 gives a comparison between the two cases with and without the static magnetic field. If no magnetic field is applied, such a system reduces to a V-type three level structure under the  $\sigma^+ - \sigma^-$  laser polarization scheme, as clearly shown in Fig.6(a), the upper Zeeman sublevel  $m'_F = 0$  always populates zero. Since the laser frequency ramps from red-detuning to blue-detuning, the counter-propagating  $\sigma^-$  beam first becomes resonant with the particle and then the co-propagating  $\sigma^+$  beam, the population imbalance between  $m'_F = -1$  and  $m'_F = +1$  sublevels in time ordering induces the cooling force.

Once introducing an angled magnetic field, the upper three sublevels simultaneously become populated as the Zeeman splitting  $\Delta_z = g_{F'} \mu_B B / \hbar$  is much smaller than the Doppler shift  $\Delta_D$  for the case in Fig.6(b). The photon scattering processes are also different from the case without a magnetic field. Here the stimulated emissions indeed occur but get depressed by the simultaneous excitations. For example, when the frequency of the co-propagating beam

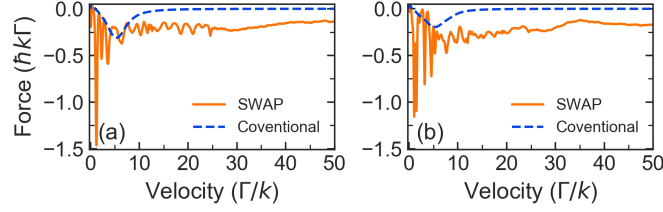


FIG. 7. Effect of the SWAP cooling on the type-II transitions: (a)  $F = 1 \rightarrow F' = 1$  and (b)  $F = 2 \rightarrow F' = 1$ . For the SWAP cooling in the both two cases, the on-resonance Rabi frequency  $\Omega = 50\Gamma$ , the frequency ramp speed  $\alpha = 100\Gamma^2$ , the sweeping period  $T = 5\Gamma^{-1}$ , the Landé  $g$ -factor of the excited  $F' = 1$  state is  $g_{F'} = -0.202$ . In (a),  $g_F = -0.5$ , while in (b),  $g_F = 0.5$ . For the conventional Doppler cooling,  $\Omega = 5\Gamma$ ,  $\Delta = -5\Gamma$ ,  $B = 5$  G and  $\theta = \pi/2$ . The dependence of the cooling forces on the moving velocity for the SWAP cooling and conventional Doppler cooling schemes are plotted in orange solid and blue dashed lines respectively.

ramps to be resonant with the moving particle, the  $\sigma^-$  component transfers the particles in  $m'_F = -1$  sublevel back to ground state via stimulated emission. However, due to the small Zeeman splitting the  $\pi$  and  $\sigma^+$  components are near resonance and rapidly excite the particles into  $m'_F = 0, +1$  sublevels, leading to the oscillations of the populations in the three Zeeman sublevels in Fig.6(b). When the frequency ramps to be largely off-resonant, the excited particles decay back to ground state via spontaneous emission, similar to the case without a magnetic field.

Since both the two cases still depend on the spontaneous emission to guarantee the excited populations back to ground state at the beginning of each sweeping period, the average cooling force even can not reach the maximum value of the conventional radiation force,  $0.5\hbar k\Gamma$ ; see Fig.6(c). The appearance of the magnetic field slightly changes the strength of the force yet, and the coolable velocity range is still determined by the frequency sweeping range  $\Delta_T = \alpha T$ . Typically, the velocity range of the SWAP scheme is much larger than the conventional Doppler cooling [Muniz2018].

#### Appendix D: SWAP cooling on type-II $F = 1, 2 \rightarrow F' = 1$ transitions

The enhanced cooling mechanism at the small velocity region under a large enough magnetic field also validates for other type-II transitions, although the resonant positions for all possible transitions become much more complicated as the angular momentum quantum number becomes larger. Figure 7(a) shows the SWAP cooling force for the  $F = 1 \rightarrow F' = 1$  transition, the maximum achievable cooling force occurs at a velocity less than  $2\Gamma/k$  and can be as large as  $1.5\hbar k\Gamma$ , about 5 times larger than that in the conventional Doppler cooling scheme. A comparison between the SWAP cooling and the Doppler cooling for the  $F = 2 \rightarrow F' = 1$  transition is illustrated in Fig.7(b). The maximum achievable cooling force also occurs at a small velocity and also 5 times larger than the Doppler limit,  $0.2\hbar k\Gamma$ . The SWAP cooling force for both two cases in large velocity region,  $v > 10\Gamma/k$ , can be as large as  $0.2\hbar k\Gamma$ . The enhancement of the cooling forces in the SWAP scheme for all possible type-II transitions indicates that enhanced laser cooling with adiabatic passage for diatomic molecules is feasible.

#### Appendix E: Effect from the energy gaps of the four hyperfine states

Due to the energy gap (tens of MHz) between each pair of hyperfine states in molecules, the  $\Lambda$ -type transition still can not be eliminated even with a rather large magnetic field strength. Figure 8 shows the case for BaF molecule with  $B = 100$  G. Because of the Zeeman splitting, some Zeeman sublevels in different hyperfine states become near to each other, for example,  $|F = 1^{(-)}, m_F = -1\rangle$  and  $|F = 2, m_F = -1\rangle$  pairs and  $|F = 1^{(+)}, m_F = -1\rangle$  and  $|F = 1^{(-)}, m_F = 0\rangle$  pairs. Population transfer in such pairs will compete with the stimulated processes and reduce the SWAP cooling effect.

On the other hand, the energy gaps do not allow a considerable small sweeping range  $\Delta_T$ . If we temporarily do not take the Zeeman shift into account, with a small  $\Delta_T$  less than the energy gap between  $F = 0$  and  $F = 1^{(+)}$  states, as shown in Fig.8(b), cooling laser beams for the upper two hyperfine states are always blue-detuned and thus heating effect emerges. Even including the Zeeman shift, there always exists blue-detuned sublevels that weaken the cooling force.



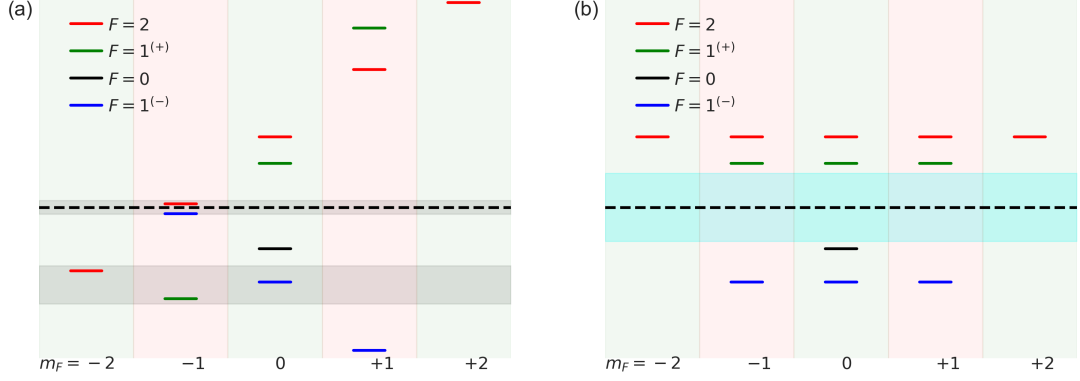


FIG. 8. Effect of the energy gaps of the four hyperfine states. (a) Under a magnetic field strength of 100 G, the Zeeman splitting make some Zeeman sublevels near each other indicated by the gray shadow region. The dashed line indicate the center frequency position of the sweeping. (b) Distribution of the energy levels without consideration on the Zeeman shift. With a small sweeping range (the cyan shaded region), the upper two hyperfine state always maintain blue-detuned.

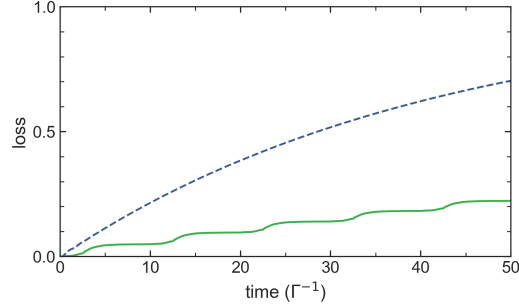


FIG. 9. Population loss to leakage channels within an evolution time of  $50\Gamma^{-1}$  in a three level system. The loss rate is 0.05. Initially, particles all populate the ground state, i.e., the loss channel vanishes. For conventional Doppler cooling (blue dashed line),  $\Omega = 5\Gamma$ . The reduced loss phenomenon for a velocity of  $v = 2\Gamma/k$  (green solid line) under the SWAP scheme ( $\Omega = 20\Gamma$ ,  $\alpha = 20\Gamma^2$ ,  $T = 10\Gamma^{-1}$ ) can be clearly figured out.

#### Appendix F: Time evolution of the loss in the SWAP cooling scheme

Figure 9 compares the population loss for the SWAP cooling scheme and that for the conventional Doppler cooling in a three-level system. Here we set the velocity of the particle as  $v = 2\Gamma/k$ . The detuning of the Doppler cooling is  $-2\Gamma$ . With an evolution time of  $50\Gamma^{-1}$ , the loss reaches  $\sim 0.7$  after scattering  $\sim 14$  photons. However, for the SWAP cooling scheme, with an equivalent evolution time, i.e., five sweeping periods, the loss is several times lower, and the loss fraction is nearly linear to the number of the sweeping period before the cooling dies.

- 
- |  |   |
|--|---|
| <p>[1] S. Chu, Rev. Mod. Phys. <b>70</b>, 685 (1998).<br/> [2] W. D. Phillips, Rev. Mod. Phys. <b>70</b>, 721 (1998).<br/> [3] C. N. Cohen-Tannoudji, Rev. Mod. Phys. <b>70</b>, 707 (1998).<br/> [4] E. A. Cornell and C. E. Wieman, Rev. Mod. Phys. <b>74</b>, 875 (2002).<br/> [5] I. Bloch, J. Dalibard, and W. Zwerger, Rev. Mod. Phys. <b>80</b>, 885 (2008).<br/> [6] A. D. Ludlow, M. M. Boyd, J. Ye, E. Peik, and P. O.</p> | <p>Schmidt, Rev. Mod. Phys. <b>87</b>, 637 (2015).<br/> [7] J. L. Bohn, A. M. Rey, and J. Ye, Science <b>357</b>, 1002 (2017).<br/> [8] M. S. Safronova, D. Budker, D. DeMille, D. F. J. Kimball, A. Derevianko, and C. W. Clark, Rev. Mod. Phys. <b>90</b>, 025008 (2018).<br/> [9] H. Metcalf, Rev. Mod. Phys. <b>89</b>, 041001 (2017).<br/> [10] T. Lu, X. Miao, and H. Metcalf, Phys. Rev. A <b>71</b>, 061405</p> |
|--|---|

- (2005).
- [11] X. Miao, E. Wertz, M. G. Cohen, and H. Metcalf, Phys. Rev. A **75**, 011402 (2007).
  - [12] A. M. Jayich, A. C. Vutha, M. T. Hummon, J. V. Porto, and W. C. Campbell, Phys. Rev. A **89**, 023425 (2014).
  - [13] J. Söding, R. Grimm, Y. B. Ovchinnikov, P. Bouyer, and C. Salomon, Phys. Rev. Lett. **78**, 1420 (1997).
  - [14] L. Yatsenko and H. Metcalf, Phys. Rev. A **70**, 063402 (2004).
  - [15] M. Partlow, X. Miao, J. Bochmann, M. Cashen, and H. Metcalf, Phys. Rev. Lett. **93**, 213004 (2004).
  - [16] C. Corder, B. Arnold, and H. Metcalf, Phys. Rev. Lett. **114**, 043002 (2015).
  - [17] E. S. Shuman, J. F. Barry, and D. DeMille, Nature **467**, 820 (2010).
  - [18] M. T. Hummon, M. Yeo, B. K. Stuhl, A. L. Collopy, Y. Xia, and J. Ye, Phys. Rev. Lett. **110**, 143001 (2013).
  - [19] M. D. Di Rosa, The European Physical Journal D - Atomic, Molecular, Optical and Plasma Physics **31**, 395 (2004).
  - [20] T. Chen, W. Bu, and B. Yan, Phys. Rev. A **94**, 063415 (2016).
  - [21] B. K. Stuhl, B. C. Sawyer, D. Wang, and J. Ye, Phys. Rev. Lett. **101**, 243002 (2008).
  - [22] T. Chen, W. Bu, and B. Yan, Phys. Rev. A **96**, 053401 (2017).
  - [23] I. Kozyryev, L. Baum, L. Aldridge, P. Yu, E. E. Eyler, and J. M. Doyle, Phys. Rev. Lett. **120**, 063205 (2018).
  - [24] H. Metcalf and P. V. der Straten, *Laser cooling and trapping* (Springer, 1999).
  - [25] J. Dalibard and C. Tannoudji, J. Opt. Soc. Am. B **6**, 2023 (1989).
  - [26] P. Ungar, D. Weiss, E. Riis, and S. Chu, J. Opt. Soc. Am. B **6**, 2058 (1989).
  - [27] M. A. Norcia, J. R. K. Cline, J. P. Bartolotta, M. J. Holland, and J. K. Thompson, New Journal of Physics **20**, 023021 (2018).
  - [28] J. A. Muniz, M. A. Norcia, J. R. K. Cline, and J. K. Thompson, arXiv: 1806.00838 (2018).
  - [29] N. Petersen, F. Mhlbauer, L. Bougas, A. Sharma, D. Budker, and P. Windpassinger, arXiv: 1809.06423 (2018).
  - [30] G. P. Greve, B. C. Wu, and J. K. Thompson, arXiv:1805.04452 (2018).
  - [31] J. P. Bartolotta, M. A. Norcia, J. R. K. Cline, J. K. Thompson, and M. J. Holland, Phys. Rev. A **98**, 023404 (2018).
  - [32] A. M. L. Oien, I. T. McKinnie, P. J. Manson, W. J. Sandle, and D. M. Warrington, Phys. Rev. A **55**, 4621 (1997).
  - [33] V. B. Tiwari, S. Singh, H. S. Rawat, and S. C. Mehendale, Phys. Rev. A **78**, 063421 (2008).
  - [34] L. Anderegg, B. L. Augenbraun, E. Chae, B. Hemmerling, N. R. Hutzler, A. Ravi, A. Collopy, J. Ye, W. Ketterle, and J. M. Doyle, Phys. Rev. Lett. **119**, 103201 (2017).
  - [35] S. Truppe, H. J. Williams, M. Hambach, L. Caldwell, N. J. F. E. A. Hinds, B. E. Sauer, and M. R. Tarbutt, Nat. Phys. **13**, 1173 (2017).
  - [36] H. J. Williams, S. Truppe, M. Hambach, L. Caldwell, N. J. Fitch, E. A. Hinds, B. E. Sauer, and M. R. Tarbutt, New Journal of Physics **19**, 113035 (2017).
  - [37] D. Wang, W. Bu, D. Xie, T. Chen, and B. Yan, J. Opt. Soc. Am. B **35**, 1658 (2018).
  - [38] K. Teng, M. Disla, J. Dellatto, A. Limani, B. Kaufman, and M. J. Wright, Review of Scientific Instruments **86**, 043114 (2015).
  - [39] B. Kaufman, T. Paltoo, T. Grogan, T. Pena, J. P. S. John, and M. J. Wright, Applied Physics B **123**, 58 (2017).
  - [40] M. Yeo, M. T. Hummon, A. L. Collopy, B. Yan, B. Hemmerling, E. Chae, J. M. Doyle, and J. Ye, Phys. Rev. Lett. **114**, 223003 (2015).